Multiple magnetic microrobot control using electrostatic anchoring

Chytra Pawashe, Steven Floyd, and Metin Sitti[a)]
Department of Mechanical Engineering, Carnegie Mellon University, Pittsburgh, Pennsylvania 15213, USA

(Received 31 January 2009; accepted 30 March 2009; published online 23 April 2009)

Addressing power and control to individual untethered microrobots is a challenge for small-scale robotics. We present a $250\times130\times100$ μm^3 magnetic robot wirelessly driven by pulsed external magnetic fields. An induced stick-slip motion results in translation speeds over 8 mm/s. Control of multiple robots is achieved by an array of addressable electrostatic anchoring pads on the surface, which selectively fixes microrobots, preventing translation. We demonstrate control of two microrobots in both uncoupled individual motion and coupled symmetric motion. An estimated anchoring force of 23.0 μN is necessary to effectively fix each microrobot. © *2009 American Institute of Physics*. [DOI: 10.1063/1.3123231]

The recent emergence of submillimeter sized robots has caused adaptations in approaches for power delivery and control at the microscale. The current designs in the literature, including electrostatic,[1,2] electromagnetic,[3–5] laser driven thermal impact,[6] and bacteria propelled systems,[7,8] have resulted in wireless control of individual mobile microrobots. However, the control of multiple microrobots presents challenges, as the power delivery and control mechanisms may not be conducive to this task. For power delivery mechanisms that rely on oscillating electric or magnetic fields, microrobots can be designed to respond differently to various actuation waveforms. This approach can allow for multiple microrobot control,[1] but thus far in the literature, the microrobots' motions are coupled to one another, requiring sophisticated algorithms to create motion paths for each microrobot. In addition, the maximum number of microrobots possible can be limited due to fabrication issues, especially since each individual robot must be mechanically different.

To enable the control of multiple microrobots in our electromagnetically actuated system,[3,4] we introduce electrostatic forces to selectively anchor microrobots to the surface. This allows for any unanchored robot to be driven by the encompassing magnetic fields, while keeping anchored robots immovable. This approach allows for the uncoupled serial actuation of each microrobot, as well as coupled parallel actuation of multiple robots. In this scheme, microrobots do not need to possess geometric differences as in other approaches.[1,5] Figure 1(a) shows a schematic displaying our multirobot motion control methodology with four microrobots.

A rectangular prismatic magnetic microrobot 250 μm long by 130 μm wide and 100 μm thick is actuated by five independent square-turn electromagnetic coils, controlled by a computer at 1 kHz bandwidth.[3,4] The microrobot is laser micromachined (Quicklaze, New Wave) out of a magnetized piece of neodymium-iron-boron, a hard magnetic material. Actuation of the microrobot is accomplished by enabling two electromagnetic coils. One of four upright coils is held at a constant current, resulting in a magnetic field of 2.3 mT at the position of the microrobot (about 50 times the Earth's magnetic field), which orients the robot on the working surface toward the coil. The magnetic force exerted by one coil is insufficient to translate the microrobot due to the relatively high friction and adhesion forces experienced on the surface. Thus, a clamping coil is activated beneath the surface, and is pulsed using a sawtooth waveform with a maximum amplitude of 2.3 mT at frequencies from 1 to 100 Hz. The resulting time-varying magnetic field causes the microrobot to rock nonuniformly, which induces stick-slip motion across the surface.[4] The robot velocity monotonically increases with pulsing frequency, exceeding 8 mm/s in air. The microrobot is also capable of operating on a variety of surfaces and in liquid environments.[4] A camera (Sony XC-75) with a microscope lens provides visual feedback of the workspace.

For multiple microrobot control, the substrate upon which the robot moves has an array of independently controlled interdigitated electrodes to provide electrostatic anchoring. A 100 nm aluminum layer is deposited onto a glass slide and patterned into the electrodes. A thin layer of SU-8 (2–7 μm) is coated onto the aluminum and is in direct contact with the microrobots. SU-8 is used because it is inexpensive and has a high dielectric strength (112 V/μm), which will support the generation of the large electric fields necessary to anchor a microrobot without damaging the substrate. For experiments, a surface with four independent electrostatic pads was fabricated. Figure 1(b) displays a free body diagram of a microrobot anchored on one pad with external forces, and a cross section of the substrate.

For the case of a conductive microrobot above an SU-8 insulation layer covering a set of interdigitated electrodes at an applied voltage difference of V_{id}, the conductor will assume a potential halfway between the two, or $\frac{1}{2}V_{id}$, if it overlaps equal areas of electrodes at both voltages.[2] With this assumption and considering negligible fringing, an estimate of the anchoring force, F_{id}, exerted by the interdigitated electrodes onto the microrobot is

$$F_{id} = \tfrac{1}{8}V_{id}^2\frac{\varepsilon_0\varepsilon_r}{g^2}A_{id}, \tag{1}$$

where A_{id} is the area of the electrodes overlapping the microrobot, g is the insulator thickness, ε_0 is the permittivity of free space, and ε_r is the relative static permittivity of the insulating material (ε_r=4.1 for SU-8).

To affix a microrobot to the surface, the electrostatic anchoring must suppress the magnetic torque (T_y) induced rotation about its contact point with the surface. The effect of

a)Electronic mail: sitti@cmu.edu.

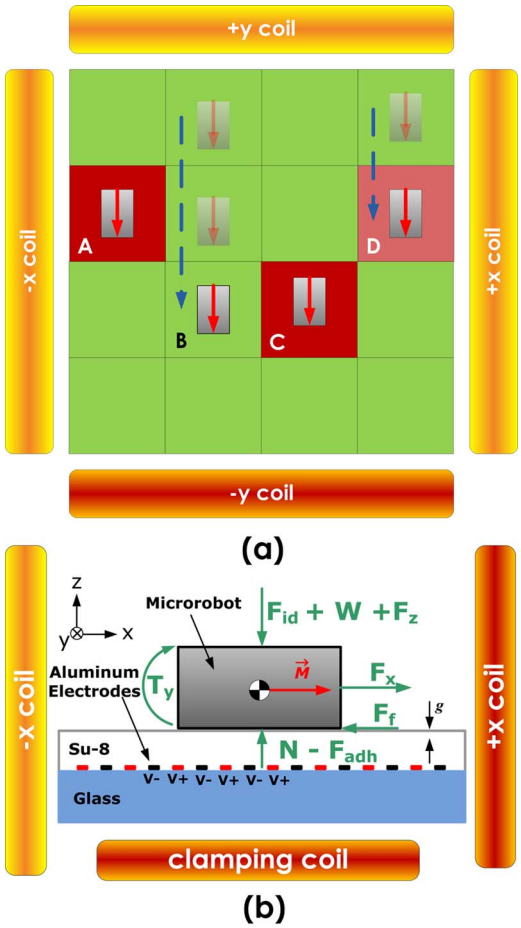

FIG. 1. (Color online) (a) Top-down schematic of four microrobots, A, B, C, and D, demonstrating coupled and decoupled motion. Each square in the 4×4 grid represents an independently controlled electrostatic anchoring pad. The $-y$ coil is enabled, causing robots to orient in the $-y$ direction. Robots A and C are anchored to the surface and do not translate. Robots B and D translate in the $-y$-direction; robot D is anchored after traversing one pad. (b) A free body diagram of an anchored magnetic microrobot experiencing an electrostatic anchoring force F_{id}, its weight W, magnetic forces F_z and F_x, magnetic torque T_y, static friction force F_f, reactive normal force N, and an adhesive force F_{adh} due to surface effects. $\vec{M}$ denotes the magnetization vector of the microrobot. The anchoring and $+x$ coils are active. The composition of the substrate is also displayed; $V-$ and $V+$ denote the relative voltage across the electrodes.

this torque significantly dominates the other interactions experienced by the microrobot, shown in Fig. 1(b). The maximum magnetic torque T_{max} that can be applied to a robot with a magnetization $\vec{M}$ at the maximum field strength $\vec{B}_{max}$ within our system is

$$T_{max} = \vec{M} \times \vec{B}_{max} = 2.88 \times 10^{-9} \ \text{N} \cdot \text{m}. \quad (2)$$

Treating the magnetic torque as a pair of forces acting in opposite directions on the ends of the microrobot, each of these forces is approximately 11.5 μN. To counteract this, the anchoring force must be approximately twice this value, as it is assumed to be evenly distributed across the bottom of the robot, and the torque about the pivot point will act at the center of the robot. Using Eq. (1) and noting that for electrodes that are 10 μm wide with 10 μm spacing, making A_{id} approximately half the apparent robot area of 250 $\times$130 μm^2, and an SU-8 thickness of $g=3.5$ μm, the required voltage is approximately 62 V.

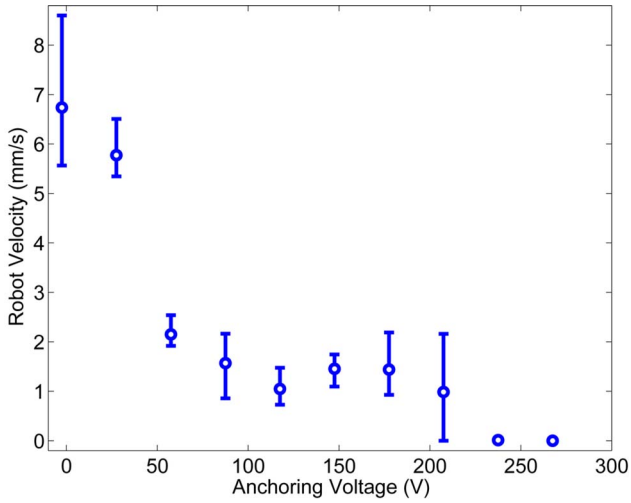

FIG. 2. (Color online) Robot velocity vs electrostatic anchoring voltage for a microrobot on a $g=3.5$ μm SU-8 layer. A critical voltage of 240 V is required to affix the microrobot. Videos of the motion were recorded and analyzed to determine velocities. A pulsing frequency of 20 Hz was used for translation. Each data point represents three measurements.

In Fig. 2, an experimental plot of microrobot velocity versus electrostatic anchoring voltage is shown. The required voltage is about 240 V to suppress robot motion. Robot velocity does not monotonically decrease as voltage is increased, but experiences a local maximum near 160 V. From stick-slip dynamic simulations, we have found that in certain regimes, increases in friction can increase robot velocity.[4] As an increased electrostatic anchoring force increases friction between the robot and surface, an increase in velocity is possible. For the purpose of multirobot control, however, only the critical voltage for effective anchoring is important.

The high voltage requirement from Fig. 2 is likely caused by a layer of air trapped between the surface asperities of the robot and SU-8. An additional air layer with thickness comparable to the robot's maximum asperity height, a, causes the total capacitance C_{tot} between the robot and the electrodes to be $C_{tot}=[C_1^{-1}+C_2^{-1}]^{-1}$, where C_1 is the capacitance associated with the SU-8 $[C_1=(\varepsilon_0\varepsilon_r/g)A_{id}]$ and C_2 is associated with the air gap $[C_2\cong(\varepsilon_0/a)A_{id}]$. Using the principal of virtual work and successive application of the chain rule for differentiation, the electrostatic anchoring force with an air gap, $F_{id,ag}$, will be

$$F_{id,ag} = \tfrac{1}{16} V_{id}^2 C_{tot}^2 \left[\frac{1}{C_1 g} k + \frac{1}{C_2 a}(1-k) \right], \quad (3)$$

where k is a constant $(0<k<1)$ relating the amount of virtual SU-8 displacement that occurs per unit of total virtual displacement. Assuming $V_{id}=240$ V and taking the limit when $k=0$ and all the contractions are in the air gap, the robot's surface roughness would be 2.45 μm. When $k=1$ and all the contractions are in the SU-8, the roughness would be 5.85 μm. A microrobot surface roughness of 2–10 μm has been experimentally observed, thus a trapped air layer seems a likely cause for the increased value of V_{id} required for anchoring.

Experimental results are provided in Fig. 3, which shows frames from a video where two magnetic microrobots are translated both individually and simultaneously [Figs. 3(a)–3(c)], and also presents the microrobots' y-displacement

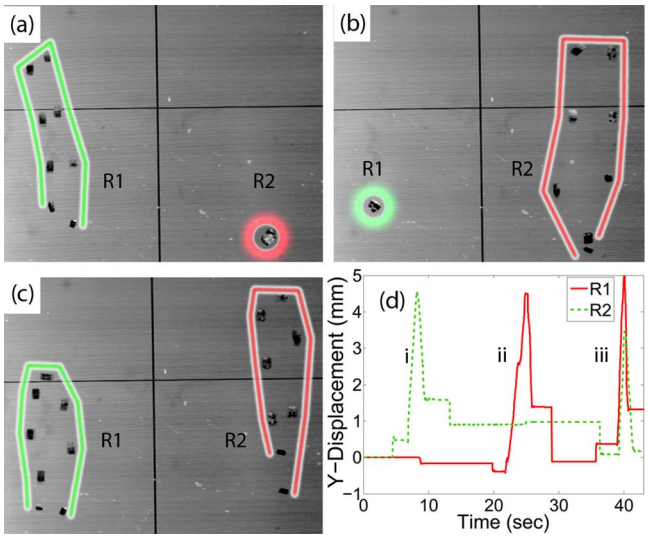

FIG. 3. (Color online) An experiment demonstrating multimicrorobot control. In (a), robot R1 (green) moves while robot R2 (red) is fixed. In (b), R2 moves while R1 is fixed. In (c), both robots move together. In (d), a plot of the y displacement vs time for each microrobot is shown, with regions i, ii, and iii corresponding to the motions in (a), (b), and (c), respectively. Each image in (a)–(c) represents an 8.6 mm wide by 6.3 mm tall area. An SU-8 thickness of $g=3.5$ μm is used, with an anchoring voltage of 260 V. The cross near the middle is the electrical separation between the four anchoring pads. A pulsing frequency of 20 Hz is used for translation.

as a function of time [Fig. 3(d)] (see video online[9]). Decoupling in position is demonstrated, however, coupling in orientation is nearly unavoidable due to the strong magnetic torque exerted in the z-direction on the microrobots; thus both anchored and unanchored microrobots rotate in the z-axis simultaneously. However, the added electrostatic force prevents the anchored robot from effectively rocking on the surface, suppressing any stick-slip translation. Discontinuities in a microrobot's position occur whenever its $\vec{M}$ is initially parallel to the substrate and the electromagnetic clamp is engaged, or $\vec{M}$ is orthogonal to the substrate and the electrostatic anchor is engaged.

As two permanent magnets will snap together at a critical distance, a minimum inter-robot spacing is necessary, on the order of several robot body lengths. For effective multi-robot cooperation, no two robots should ever be within this range of each other. The maximum size of the electrostatic pads should be comparable to this distance as well; any larger, and one cannot effectively utilize the entire working area. Smaller pads may be preferable for finer control of the anchoring area, but introduce increased hardware complexity. Regardless of the electrostatic pad size, sufficient area must be activated to ensure anchoring of a robot at all orientations and account for any drift. In addition, to decrease the snap-into-contact distance, robots with lower magnetization values can be utilized; this will be presented in future work.

In summary, we demonstrate that electrostatic coupling to a substrate can facilitate multirobot control for untethered magnetic microrobots. Two microrobots were shown to be uncoupled from each other in position, and can be translated independently of each other in the presence of a global driving magnetic field. An estimated anchoring force of 23.0 μN was necessary to effectively fix a microrobot. Future works will include increasing the number of electrostatic anchoring pads and robots, and developing algorithms to control the motion of an arbitrary number of microrobots autonomously.

The authors thank the members of the NanoRobotics Laboratory for all their support and suggestions. This work is supported by the National Science Foundation CAREER award program (Grant No. NSF IIS-0448042).

[1]B. R. Donald, C. G. Levey, and I. Paprotny, J. Microelectromech. Syst. **17**, 789 (2008).
[2]B. Donald, C. Levey, C. McGray, D. Rus, and I. Paprotny, J. Microelectromech. Syst. **12**, 947 (2003).
[3]S. Floyd, C. Pawashe, and M. Sitti, *Proceedings of IEEE Conference on Robotics and Automation* (IEEE, Pasadena, CA, 2008), p. 419.
[4]C. Pawashe, S. Floyd, and M. Sitti, Proceedings of Robotics Science and Systems IV, Zurich, Switzerland, 2008, http://www.roboticsproceedings.org/rss04/p37.html.
[5]K. Vollmers, D. Frutiger, B. Kratochvil, and B. Nelson, Appl. Phys. Lett. **92**, 144103 (2008).
[6]O. Sul, M. Falvo, R. Taylor, S. Washburn, and R. Superfine, Appl. Phys. Lett. **89**, 203512 (2006).
[7]B. Behkam and M. Sitti, Appl. Phys. Lett. **93**, 223901 (2008).
[8]S. Martel, C. Tremblay, S. Ngakeng, and G. Langlois, Appl. Phys. Lett. **89**, 233904 (2006).
[9]See EPAPS Document No. E-APPLAB-94-089916 for a video demonstrating multiple microrobot motion. For more information on EPAPS, see http://www.aip.org/pubservs/epaps.html.